Ductility reduction factor formulations for seismic design of RC wall and frame structures

Matteo Zerbin[1,*], Alessandra Aprile[1], Katrin Beyer[2] and Enrico Spacone[3]

[1]*Engineering Department, University of Ferrara, via Saragat 1, 44122 Ferrara, Italy*

[2]*Earthquake Engineering and Structural Dynamics, École Polytechnique Fédérale de Lausanne, 1015 Lausanne, Switzerland*

[3]*Department of Engineering and Geology, University of Chieti-Pescara, viale Pindaro 42, 66100 Pescara, Italy*

ABSTRACT

Seismic design of standard structures is typically founded on a force-based design approach. Over the years this approach has proven robust and easily applicable by design engineers and – in combination with capacity design principles – it provides a good protection against premature structural failures. However, it is also known that the force-based design approach as it is implemented in the current generation of seismic design codes suffers from some shortcomings; among these is the fact that the base shear is computed using a pre-defined force reduction factor, which is constant for a given structural system. Thus, for the same design input, structures of an identical type but different geometry are subjected to varying ductility demands and may perform differently during an earthquake. The objective of this research is to present an alternative formulation for computing force reduction factors for RC wall and frame structures, using simple analytical models which only require input data already available at the beginning of the design process. Such analytical models allow to link global to local ductility demands and therefore to compute an estimate of the force ductility reduction factors that lead to equal local ductility demands and expected damage levels. A series of pushover and nonlinear time history analyses are run on simplified numerical models of a set of wall and frame structures. The results show that the proposed alternative formulation yields a more accurate ductility reduction factor than the current Eurocode 8 design approach.

Received ; Revised ; Accepted

KEYWORDS: RC wall structures, RC frame structures, ductility reduction factor, force-based seismic design, pushover analysis, nonlinear dynamic analysis

Declarations of interest: none

1. Introduction

Reinforced concrete (RC) structures are typically supported by walls or frames to resist both gravity and horizontal loads. Nowadays, the Force-Based Design (FBD) approach is the standard method to design structures for seismic loads. Because a linear elastic analysis is required, over the years this approach has proven to be both robust and easily applicable by design engineers. Inelastic behavior is implicitly considered through the force reduction factor or behavior factor.

In early earthquake engineering works, Biot [1] introduced the formulation of what would later become known as the Response Spectrum Method (RSM), Housner [2] attempted to combine the response spectrum and the dissipation of seismic energy through plastic deformations and Veletsos and Newmark [3] started

* Corresponding author. Tel.: +39 3480382670.
E-mail addresses: matteo.zerbin@unife.it (M. Zerbin), alessandra.aprile@unife.it (A. Aprile), katrin.beyer@epfl.ch (K. Beyer), enrico.spacone@unich.it (E. Spacone).

to study inelastic spectra for elastic-perfectly plastic structures. To the authors' knowledge, the force reduction factor firstly appeared in the Blue Book [4] in an attempt to unify the design approaches providing minimum safety standards for structures. Before the Blue Book [4], the Uniform Building Code [5] computed the total base shear and the lateral force distribution without any consideration of the structural system type. The 1959 edition of the Blue Book [4] introduced a force reduction factor called "K factor" to account for the different structural system type and redefined the "C factor", a horizontal force factor depending on the structure fundamental period.

Seismic codes have been under constant evolution since 1959 and current building codes require a force-based approach for limit state design. This allows structures' performance to be verified on two levels of seismic intensities, corresponding to the ultimate limit state (ULS) and the serviceability limit state (SLS). Furthermore, the designer, via capacity design principles, can control the failure mechanism and avoid the formation of local mechanisms and premature brittle failures of the structural elements [6]. The strength and energy-dissipation capacity assigned to the structure are related to the exploitation of its non-linear response.

The value of the force reduction factor depends on structure's ductility, as well as its internal strength reserves, in turn this depends mainly on its structural redundancy, on the individual members' overstrength and on the structure's damping [7]. All these factors directly affect the structure's energy dissipation capacity. The ATC-19 [8] suggests a general definition of the force reduction factor in the following form:

$$\mathrm{R} = R_\mu R_s R_\zeta \approx R_\mu R_s \tag{1}$$

where R_μ is the ductility-dependent component, R_s the overstrength-dependent component, and R_ζ the damping-dependent component of the force reduction factor, which is usually neglected by codes unless the structures have supplemental damping devices. A separate factor relating to the structural redundancy only, R_r, is sometimes added, but it is usually included beforehand [8].

The ductility reduction factor for a SDOF system, $R_{\mu,SDOF}$, is defined as the ratio between the peak force in an elastic system $V_{b,SDOF}(\mu = 1)$ and the peak force $V_{b,SDOF}(\mu = \mu^*)$ in an elastic-perfectly plastic oscillator with identical elastic period, damping and mass, for a given target displacement ductility, μ^* ([9], [10]):

$$R_{\mu,SDOF} = \frac{V_{b,SDOF}(\mu = 1)}{V_{b,SDOF}(\mu = \mu^*)} \tag{2}$$

The displacement ductility is defined as the ratio of the maximum displacement demand divided by the yield displacement. In SDOF systems, the top displacement ductility μ, the interstorey drift ductility μ_{IDR} and the storey displacement ductility μ_Δ are identical. Here below, the ductility of MDOF frame systems will be defined as interstorey drift ductility μ_{IDR}, where the interstorey drift ratio (IDR) is defined as the difference between displacements at storeys i and $i-1$, Δ_u, divided by the storey height, h_s. This solution has been chosen as a more practical parameter for engineers than μ_Δ. Other authors ([9], [10]) opted to assess frame structures' ductility by assuming the same values whereby the interstorey drift ratio is equal to the storey displacement divided by the storey height. Thus:

$$\mu_{IDR} = \frac{IDR_u}{IDR_y} = \frac{\frac{\Delta_u}{h_s}}{\frac{\Delta_y}{h_s}} = \frac{\Delta_u}{\Delta_y} = \frac{d_{u,i} - d_{u,i-1}}{d_{y,i} - d_{y,i-1}} = \mu_\Delta \quad \overset{SDOF\ system}{\Rightarrow} \quad \mu_{IDR} = \mu_\Delta = \mu = \frac{d_u}{d_y} \tag{3}$$

In a real MDOF building, higher mode effects induce a base shear demand, $V_{b,MDOF}$ larger than that of its equivalent SDOF system, $V_{b,SDOF}$, with an elastic period corresponding to the MDOF system's fundamental persiod [11]. The ratio of the two base shears is the shear magnification factor, ε:

$$\varepsilon = \frac{V_{b,MDOF}(\mu = \mu^*)}{V_{b,SDOF}(\mu = \mu^*)} \tag{4}$$

Its inverse is the modification factor, R_M [9], [10]:

$$R_M = \frac{1}{\varepsilon} = \frac{V_{b,SDOF}(\mu = \mu^*)}{V_{b,MDOF}(\mu = \mu^*)} \tag{5}$$

The force reduction factor of a MDOF system can thus be written as the product of the SDOF system's force reduction factor, $R_{\mu,SDOF}$, multiplied by the modification factor, R_M, that takes into account the base shear's amplification due to higher mode effects:

$$R_{\mu,MDOF} = \frac{V_{b,SDOF}(\mu = 1)}{V_{b,MDOF}(\mu = \mu^*)} = \frac{V_{b,SDOF}(\mu = 1)}{V_{b,SDOF}(\mu = \mu^*)} \cdot \frac{V_{b,SDOF}(\mu = \mu^*)}{V_{b,MDOF}(\mu = \mu^*)} = R_M R_{\mu,SDOF} \tag{6}$$

This study does not address the overstrength-dependent component, R_s, of the force reduction factor which for the purpose of this work is evaluated via nonlinear static analyses (pushover analysis) in Section 5. Detailed information on the overstrength of RC systems can be found in [12], [13], [14].

Several expressions have been proposed for the ductility reduction factor of SDOF systems; the most relevant are found in [15], [16], [17], [18], [19], [20], [21], [22], [23], [24], [25], [26], [27]. These studies concluded that the two main parameters governing the ductility reduction factor are the displacement ductility and the system's fundamental period. A review and comparison of these works is presented in detail by Miranda and Bertero [28].

Nassar and Krawinkler [20] proposed an expression for $R_{\mu,SDOF}$ that was derived from regression analysis of the numerical responses of SDOF nonlinear systems when subjected to 15 ground motions. They examined the ductility reductions factor's sensitivity to the natural period, the yield force, the strain hardening ratio and the hysteretic model was examined. The result was the following expression was given for the mean value of the ductility reduction factor:

$$R_{\mu,SDOF} = (c(\mu - 1) + 1)^{\frac{1}{c}}; \quad c = \frac{{T_1}^a}{1 + {T_1}^a} + \frac{b}{T_1} \tag{7}$$

where T_1 is the fundamental period and parameters a and b are functions of the rate α, i.e. the ratio, expressed as percentage, of the system's post-yield stiffness to its initial stiffness. Parameters a and b are given in [20].

To the current authors' knowledge, the relationship between MDOF and SDOF system responses was first studied by Veletsos and Vann [29]. Nassar and Krawinkler [20] examined three types of simplified MDOF models. The goal was to estimate the modifications required to the inelastic strength demands obtained from bilinear SDOF systems in order to limit, to a prescribed value, the storey ductility demand in the first storey of the MDOF systems. The study concluded that MDOF ductility demands differ significantly from those of the corresponding SDOF systems and that the failure mechanism strongly affects the force reduction factor. The amplification of the base shear in MDOF systems with respect to that of SDOF systems was studied by Chopra [11], who observed that: (i) the modification factor decreases as the building fundamental period increases, and thus as the number of storeys increases; (ii) the modification factor decreases as the system ductility increases. Other relevant works on this topic are [30], [31], [9], [10], [32], [33].

Building codes typically define constant force reduction factors for a given structural system type. As a result, for the same design input, structures of the same structural system type, but different plan and elevation geometry, are subjected to different ductility demands and may, therefore, perform differently during the same earthquake. Eurocode 8 [34] defines force reduction factors – or behavior factors q – for RC buildings as the product of a basic behavior factor q_0 (that depends on the structural system type and on its regularity in elevation) and the α_u/α_1 ratio that represents the overall structural overstrength. The Italian Building Code [35] follows the same definition and the same values of Eurocode 8 [34] for RC structures. The ASCE SEI 7-10 [36] prescribes force reduction factors for several structural systems. The force reduction factors depend on the structural elements' performance; ordinary, intermediate and special elements are expected to withstand minimal, moderate and significant inelastic behavior, respectively. The stringency of the detailing requirements is related to the expected behavior. It can be observed that the other

main international building codes ([37], [38], [39]) approach the FBD seismic design method with similar definitions of the force reduction factor.

This paper intends to present an alternative formulation for computing force reduction factors for RC wall and frame structures, using simple analytical models that only require input data already available at the beginning of the design process instead of the conventional numerical procedure, as shown in Section 3. The main goal of this study is to provide a more appropriate behavior factor to be used for design based on linear analysis. The proposed formulation has the main advantage of being simpler and less costly than more advanced design methods based on pushover and nonlinear time history analyses. This study is limited to structures that are regular in plan and in elevation. Section 2 presents the proposed analytical models for alternative formulation of force reduction factors concerning wall and frame systems. Section 3 describes the numerical analyses for the validation of the alternative formulation and ductility reduction factor computation. Section 4 reports the analyses' results. Section 5 shows a comparison between the results of the proposed formulation and the values provided by Eurocode 8 [34]. Finally, Section 6 presents the main conclusions of this study.

2. Analytical models for alternative formulation of force reduction factors

The proposed analytical formulation is aimed to obtain the force reduction factors by means of a simplified model, which is able to transform and simplify the real structure – an MDOF system – into an equivalent SDOF system. Floors are considered as rigid diaphragms, thus the number of degrees of freedom is equal to the number of storeys n_s. To obtain the properties of the equivalent SDOF the procedure followed is the one proposed by Chopra [40], which is based on the following assumptions for the systems' free vibration: (i) equal elastic base shear; (ii) equal elastic base moment; (iii) equal kinetic energy; (iv) equal fundamental period; (v) equal damping ratio between SDOF system and MDOF systems.

The present work only takes into consideration the equivalent SDOF system corresponding to the first mode. To compensate for taking only one mode into account, the equivalent mass of the SDOF system, m^*, is defined as equal to the total mass of the MDOF system. This assumption follows [11], [9] for the calculation of the modification factor, R_M. Thus, when regular buildings are considered, the SDOF system better approximates the total base shear of MDOF system when regular buildings are considered. The current study only examines structures that are regular in plan and elevation, so the first mode's equivalent mass is dominant compared to the equivalent mass of other modes and it is considered sufficient to represent the system's displacement response. Here it's important to point out that most building codes use a similar approach, i.e. they compute the base shear starting using the total weight of the structures in the simplified linear static analysis.

The effective height of the equivalent SDOF system, h^*, can be written as:

$$h^* = {h_1}^* = \frac{\sum_{i=1}^{n_s} m_i \phi_i h_i}{\sum_{i=1}^{n_s} m_i \phi_i} \tag{8}$$

where m_i, ϕ_i, h_i are the storey mass, the first mode displacement, and the height from ground level, respectively, of the *i-th* storey. The effective linear stiffness of the SDOF system, k^*, is:

$$k^* = \frac{4\pi^2 m^*}{{T_1}^2} \tag{9}$$

where m^* is the total mass and T_1 is the fundamental period of the building

2.1. Wall structures

The proposed analytical model for wall structures consists of a single linear elastic cantilever beam with a rotational plastic hinge at the base. Wall structures are assumed to be dominated by flexural deformations.

For the sake of simplicity, this study assumes, in plan and elevation regular structures with a constant storey mass, $m_{s,w}$, and a constant storey height, h_s, are assumed but the method is general and applicable to structures with different storey weights and storey heights. The building has n_s storeys and the total building height is H_w. An analytical estimation of the fundamental period of a pure-flexural cantilever wall, $T_{1,w}$, can be found in [41]:

$$T_{1,w} = \frac{2\pi}{3.516}\sqrt{\frac{m_{l,w}}{EI_{w,y}}}{H_w}^2 \tag{10}$$

where $m_{l,w}$ and $EI_{w,y}$ are the mass per unit height and the yield flexural stiffness of the wall, respectively. The stiffness $EI_{w,y}$ is the effective flexural stiffness, defined as the ratio of the yield moment, $M_{y,w}$, to the yield curvature of the base section of the wall, $\varphi_{y,w}$.

The plastic hinge length, $L_{p,w}$, is defined as suggested in [42] and recommended by [6]:

$$L_{p,w} = \max\left\{0.2\left(\frac{f_u}{f_y} - 1\right)L_{s,w} + 0.2l_w + L_{sp,w}; 2L_{sp,w}\right\} \tag{11}$$

with:

$$L_{s,w} = h_G = \frac{\sum_{i=1}^{n_s} F_i h_i}{\sum_{i=1}^{n_s} F_i} \Rightarrow \frac{2n_s + 1}{3n_s} H_w; \quad L_{sp,w} = 0.022 f_y d_{bl,w} \tag{12}$$

where: $L_{s,w}$ and $L_{sp,w}$ are the shear span length and the strain penetration length, respectively; f_y and f_u are the steel yield stress and the steel tensile strength, respectively; $d_{bl,w}$ is the maximum rebar diameter in the base section of the wall and l_w is the section length. The plastic hinge is graphically shown in Figure 1(a). The shear span length calculated by Equation (12) assumes an inverse triangular load distribution of horizontal forces, F_i, applied at storey heights, h_i, as shown in Figure 1(b).

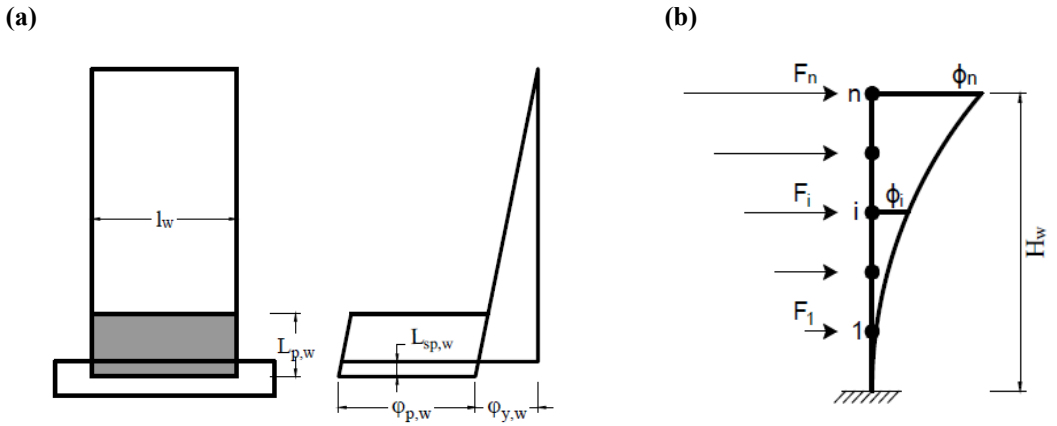

Figure 1: (a): Assumed curvature distribution of a wall that formed a flexural plastic hinge at the base, (b): Inverse triangular horizontal forces and corresponding wall displacement shape.

Predicting the ductility reduction factor of the MDOF system requires estimates of the ductility reduction factor of the corresponding SDOF system and the modification factor are needed. The following calculation derives an analytical model for the equivalent SDOF system representing the wall system is derived. The first-mode shape, necessary to define the equivalent SDOF system, is estimated using the expression proposed by [42] and assuming an inverse triangular load distribution of horizontal forces, as shown in Figure 1(b):

$$\phi_{i,w} = \frac{3}{2}\frac{{h_i}^2}{{H_w}^2}\left(1 - \frac{h_i}{3H_w}\right) \tag{13}$$

where $\phi_{i,w}$ is the wall structure first mode displacement at the *i-th* storey. The equivalent SDOF system's yield base shear, ${V_{y,w}}^*$, the ultimate base shear, ${V_{u,w}}^*$, the yield displacement, ${d_{y,w}}^*$, are, respectively:

$${V_{y,w}}^* = \frac{M_{y,w}}{{h_w}^*}; \quad {V_{u,w}}^* = \frac{M_{u,w}}{{h_w}^*}; \quad {d_{y,w}}^* = \frac{{V_{y,w}}^*}{{k_w}^*} \tag{14}$$

where $M_{y,w}$ and $M_{u,w}$ are the yield and ultimate moment of the wall base section, respectively; ${h_w}^*$ and ${k_w}^*$ are calculated using Equation (8) and (9). The equivalent yield curvature, ${\varphi_{y,w}}^*$, for the equivalent SDOF system is:

$${\varphi_{y,w}}^* = \frac{3M_{y,w}}{{k_w}^*{{h_w}^*}^3} \tag{15}$$

In order to obtain the same sectional ductility of wall's plastic hinge, $\mu_{\varphi,w}$, in the SDOF and MDOF systems, the ultimate curvature of the SDOF system, ${\varphi_{u,w}}^*$, is written as:

$${\varphi_{u,w}}^* = \mu_{\varphi,w}{\varphi_{y,w}}^* = \frac{\varphi_{u,w}}{\varphi_{y,w}}{\varphi_{y,w}}^* \tag{16}$$

where $\varphi_{y,w}$ and $\varphi_{u,w}$ are the yield and ultimate curvature of the wall base section, respectively. The plastic displacement, ${d_{p,w}}^*$, ultimate displacement, ${d_{u.w}}^*$, and displacement ductility, ${\mu_w}^*$, for the SDOF system are then given by:

$${d_{p,w}}^* = \left({\varphi_{u,w}}^* - {\varphi_{y,w}}^*\right)L_{p,w}{h_w}^*; \quad {d_{u,w}}^* = {d_{y,w}}^*\frac{{V_{u,w}}^*}{{V_{y,w}}^*} + {d_{p,w}}^* \tag{17}$$

$${\mu_w}^* = \frac{{d_{u,w}}^*}{{d_{y,w}}^*} \tag{18}$$

Once the structural ductility ${\mu_w}^*$ is known, the force reduction factor for the equivalent SDOF system, $R_{\mu,SDOF,w}$, can be estimated from Equation (7). Finally, the ductility reduction factor for the MDOF system wall structure, $R_{\mu,MDOF,w}$, is given by the following expression:

$$R_{\mu,MDOF,w} = R_{M,w}R_{\mu,SDOF,w} \tag{19}$$

where the modification factor $R_{M,w}$ is introduced to take into account higher mode effects for wall structures. Following Priestley *et al*. [42] the amplified base shear for walls is:

$$V_{b,MDOF,w} = \phi^0 \omega_{v,Ti} V_{b,SDOF,w} = \phi^0 \left(1 + \frac{{\mu_w}^*}{\phi^0} c_{2,Tw}\right) V_{b,SDOF,w} \tag{20}$$

$$c_{2,Tw} = 0.067 + 0.4(T_{1,w} - 0.5) \quad \begin{cases} \leq 1.150 \\ \geq 0.067 \end{cases} \tag{21}$$

where ϕ^0 is the overstrength factor that relates the maximum feasible flexural strength to the design strength. ϕ^0 is set equal to 1 because this study assumes the mean values of the material properties instead of the design ones are assumed. This method is validated by [42] for the following displacement ductility and fundamental period ranges, respectively: $1 \leq {\mu_w}^* \leq 7$; $0.5\ s \leq T_{1,w} \leq 3.9\ s$. The modification factor for wall structures, $R_{M,w}$, is thus assumed equal to:

$$R_{M,w} = \frac{V_{b,SDOF,w}}{V_{b,MDOF,w}} = \frac{1}{\phi^0 \omega_{v,Ti}} \tag{22}$$

2.2. Frame structures

The proposed analytical model for frame structures consists of a linear elastic one-storey/one-column shear frame with two rotational plastic hinges, one at the base and one at the top of the column (Figure 2(a)). Adjustments are made to account for higher mode effects.

Similarly to wall systems, frame structures are assumed to have a constant storey mass, $m_{s,f}$, and a constant storey height, h_s. An analytical estimation of the fundamental period of a pure-shear cantilever, $T_{1,f}$, can be found in [41]:

$$T_{1,f} = 4\sqrt{\frac{m_{l,f}}{12EI_{f,y}}} h_s H_f \tag{23}$$

where $m_{l,f}$ and $EI_{f,y}$ are respectively the mass per unit height and the base column yield flexural stiffness defined as the ratio between the yield moment, $M_{y,f}$, and the yield curvature of the frame's base column, $\varphi_{y,f}$; the total building height is H_f.

The plastic hinge length, $L_{p,f}$, is defined as suggested by [42]:

$$L_{p,f} = 0.08h_s + L_{sp,f} = 0.08h_s + 0.022 f_y d_{bl,f} \tag{24}$$

where $L_{sp,f}$ is the strain penetration length; h_s is the storey height; $d_{bl,f}$ is the maximum rebar diameter in the frame's base columns, respectively. Plastic hinges are graphically shown in Figure 2(a). The case of inverse triangular distribution of horizontal forces, F_i, applied at storey heights, h_i, is shown in Figure 2(b).

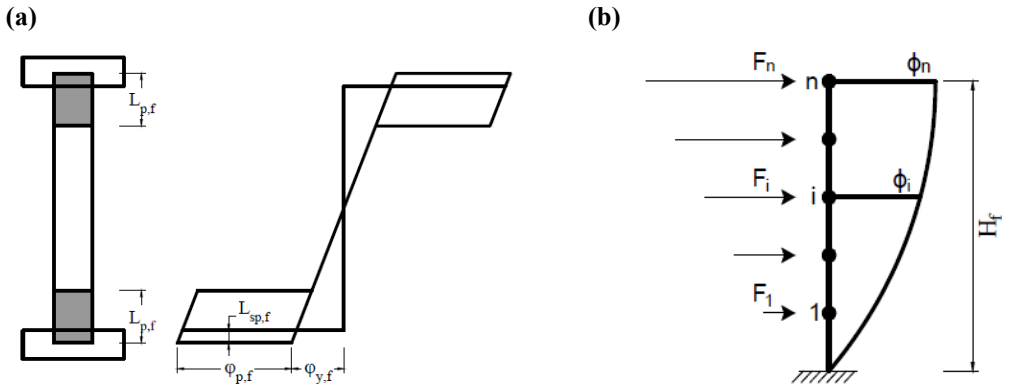

Figure 2: (a): Plastic hinges for frames, (b): Inverse triangular horizontal forces and corresponding frame displacement shape.

Similarly to wall systems, the analytical model for frame systems is based on an equivalent SDOF system able to predict the ductility reduction factor of the MDOF system, $R_{\mu,MDOF,f}$, through a modification factor, $R_{M,f}$. The elastic displacement shape of frame structures is estimated using the expression proposed by [42] and assuming an inverse triangular distribution of horizontal forces, as shown in Figure 2(b). In this case:

$$\phi_{i,f} = \frac{4\,h_i}{3H_f}\left(1 - \frac{h_i}{4H_f}\right) \tag{25}$$

where $\phi_{i,f}$ is the frame's first mode displacement of the *i-th* storey. The yield base shear, ${V_{y,f}}^*$, the ultimate base shear, ${V_{u,f}}^*$, the yield displacement, ${d_{y,f}}^*$, of the equivalent SDOF system are:

$${V_{y,f}}^* = \frac{M_{y,f}}{h_s/2}; \quad {V_{u,f}}^* = \frac{M_{u,f}}{h_s/2}; \quad {d_{y,f}}^* = \frac{{V_{y,f}}^*}{{k_f}^*} \tag{26}$$

where $M_{y,f}$ and $M_{u,f}$ are the yield and ultimate moment of the frame base column, respectively; ${k_f}^*$ is calculated using Equation (9). The yield displacement, ${d_{y1,f}}^*$, and the plastic displacement, ${d_{p1,f}}^*$, for the first storey of the MDOF system are given by:

$${d_{y1,f}}^* = \frac{{V_{y,f}}^*}{12EI_f/{h_s}^3}; \quad {d_{p1,f}}^* = (\varphi_{u,f} - \varphi_{y,f})L_{p,f}h_s \tag{27}$$

where $\varphi_{y,f}$ and $\varphi_{u,f}$ are the yield and ultimate curvature of the base column of the frame, respectively. In order to have the same plastic displacement for the equivalent SDOF system, ${d_{p,f}}^*$, the plastic displacement first storey of the MDOF, ${d_{p1,f}}^*$, is:

$${d_{p,f}}^* = \frac{{d_{p1,f}}^*}{{d_{y1,f}}^*}{d_{y,f}}^* \tag{28}$$

The ultimate displacement, ${d_{u,f}}^*$, and the displacement ductility, ${\mu_f}^*$, for the equivalent SDOF system are then given by the following expressions:

$$d_{u,f}{}^{*} = d_{y,f}{}^{*}\frac{V_{u,f}{}^{*}}{V_{y,f}{}^{*}} + d_{p,f}{}^{*} = d_{y,f}{}^{*}\frac{M_{u,f}}{M_{y,f}} + d_{p,f}{}^{*} \tag{29}$$

$$\mu_{f}{}^{*} = \frac{d_{u,f}{}^{*}}{d_{y,f}{}^{*}} \tag{30}$$

Once the structural ductility, $\mu_{f}{}^{*}$, is known, the force reduction factor for the equivalent SDOF system, $R_{\mu,SDOF,f}$, can be estimated using (7). Finally, the ductility reduction factor for MDOF system of frame structures, $R_{\mu,MDOF,f}$, is given by the following expression:

$$R_{\mu,MDOF,f} = R_{M,f}R_{\mu,SDOF,f} \tag{31}$$

where the modification factor, $R_{M,f}$, accounts for the frame's higher mode effects. A method to assess higher mode effects for frame structures is proposed by Priestley *et al*. [42], defining the amplified base shear for frames as:

$$V_{b,MDOF,f} = \omega_{v,\mu}V_{b,SDOF,f} = \left(\phi^{0} + 0.1\mu_{f}{}^{*}\right)V_{b,SDOF,f} \tag{32}$$

where ϕ^{0} is the overstrength factor relating the maximum feasible flexural strength to design strength; in this work ϕ^{0} is equal to 1 because mean values of material properties are assumed instead of design ones. Equation (32) was obtained from nonlinear time history analyses of RC frame structures designed according to the Direct Displacement Based Design, DDBD, [42], but it can be considered valid also for shear frames. With regard to the failure mechanism that they form, shear frames differ from DDBD frames that are developed using capacity design principles Shear frames represent weak column – strong beam structures while capacity designed structures are designed to form a strong column – weak beam mechanism. The modification factor for frame structures, $R_{M,f}$, is defined equal to:

$$R_{M,f} = \frac{V_{b,SDOF,f}}{V_{b,MDOF,f}} = \frac{1}{\omega_{v,\mu}} \tag{33}$$

3. Numerical analyses for the validation of the alternative formulation and ductility reduction factor computation

In this section numerical analyses for the validation of the alternative formulation for wall and frame structures are presented and the iterative procedure followed to compute the ductility reduction factor is reported in detail. The software used to perform the numerical analyses is the open-source software OpenSees [43], [44]. Pre-processing and post-processing of data were conducted with the software MATLAB [45].

3.1. Wall structures

The MDOF wall system is modelled as a flexural cantilever beam. The numerical model takes a single wall as representative of the entire wall system. The cantilever is modelled as an Euler-Bernoulli elastic beam with rigid-plastic rotational springs at the wall base and at each storey level, as shown in Figure 3(a). Masses are assigned to each floor level. The flexural stiffness of the wall is equal to the ratio of the yield moment, $M_{y,w}$, to the yield curvature, $\varphi_{y,w}$ [42].

The rotational springs' moment-rotation relationship is assumed as bilinear for the sake of simplicity and to limit the computational time. The rotational springs are modelled as zero-length elements in OpenSees [43] with the uniaxial bilinear material "Steel01". The rigid-plastic hinge is modelled with the initial elastic tangent stiffness, $k'_{\theta} = 1000k_{\theta}$, where k_{θ} is the flexural stiffness of the elastic cantilever

(since OpenSees does not include rigid-elastic material), as well as with the post-yield hardening stiffness, $b'_\theta = b_\theta$, which are calculated with corresponding moment to rotation ratios. The assumed properties of the bilinear moment-rotation hinges are described here below and are illustrated in Figure 3(b).

The SDOF model consists in a single element of height, ${h_w}^*$, area, A_w, stiffness, ${k_w}^*$, and mass, ${m_w}^*$, placed on top. The properties of the bilinear moment-rotation hinge are evaluated just like the MDOF system's hinge by replacing $\varphi_{y,w}$ and $\varphi_{u,w}$ with ${\varphi_{y,w}}^*$ and ${\varphi_{u,w}}^*$, given by Equations (15) and (16). The elastic equivalent SDOF system uses the nonlinear SDOF model with a rigid-plastic base hinge.

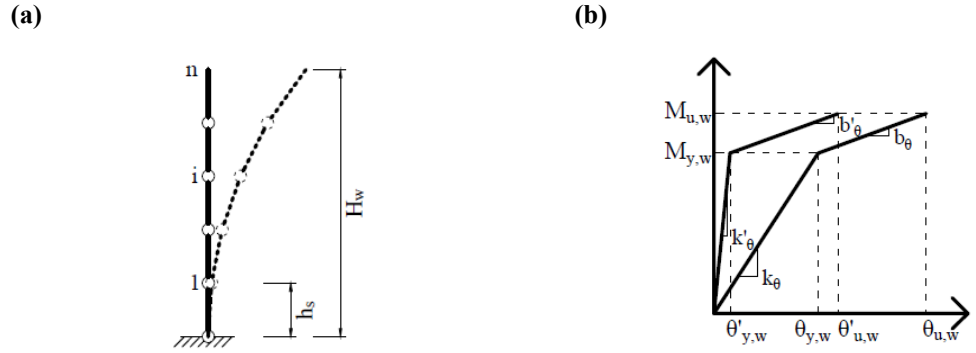

Figure 3: (a): MDOF model of wall system, (b): Plastic hinges (one with a very high elastic stiffness representative of a rigid-plastic hinge, the other elasto-plastic).

3.2. Frame structures

The MDOF frame structure is modelled as a shear frame with a single column/storey. The response of each column is lumped into a single bilinear translational spring, as shown in Figure 4(a). Masses are assigned to each floor level. Beams are defined as rigid by multiplying the material Young's modulus by $1e07$, in order to simulate a shear-type system.

The shear force-displacement relationship is assumed bilinear for the sake of simplicity and to limit computational time of nonlinear analyses. The translational springs are modelled as zero-length elements in OpenSees [43] using the uniaxial bilinear material "Steel01". The elasto-plastic hinge is modelled with the initial elastic tangent stiffness, k_Δ, the shear stiffness of the shear frame, and the post-yield hardening stiffness, b_Δ, which are calculated with corresponding shear to displacement ratios. The assumed properties of the bilinear shear force-displacement hinge are described here below and are illustrated in Figure 4(b).

The SDOF model consists of a single storey shear frame with height, ${h_f}^*$, stiffness, ${k_f}^*$, and mass, ${m_f}^*$ placed on top. The elastic equivalent SDOF system uses the nonlinear SDOF model with a linear elastic shear-displacement hinge.

(a) **(b)**

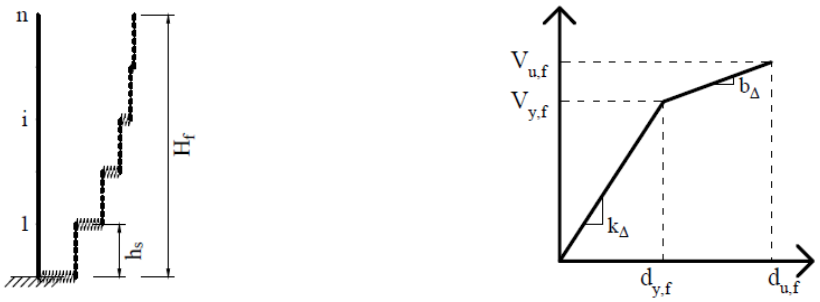

Figure 4: (a): MDOF model of frame system, (b): Bilinear moment-rotation hinge.

3.3. SDOF and MDOF ductility reduction factors computation

The procedure to calculate the reduction factor for wall and frame systems is defined by the following steps and is graphically shown in the flowchart of Figure 5. It is based on Santa-Ana [9] and Wang *et al*. [10] works.

1) The properties of the equivalent SDOF system are defined, Equation (8)-(10).
2) For a given ground motion (GM), the base shear of the MDOF system at the maximum target ductility capacity, μ, $V_{b,MDOF,w}(\mu = \mu_w \equiv {\mu_w}^*)$ or $V_{b,MDOF,f}(\mu = \mu_f \equiv {\mu_f}^*)$, is computed by scaling the intensity of the ground motion until the maximum rotation for walls, $\theta_{u,w,i} = \theta_{u,w,i,max}$, or until the maximum displacement for frames, $d_{u,f,i} = d_{u,f,i,max}$, is attained in one of the n_s hinges, within a 5% tolerance. The scaling factor is obtained using an iterative procedure. The MDOF wall system ductility, μ_w, is defined as the displacement ductility evaluated at the effective modal height ${h_w}^*$. At each iteration μ_w is computed as the ratio between the ultimate displacement, $d_u({h_w}^*)$, and the yield displacement, $d_y({h_w}^*)$:

$$\mu_w = \mu = \frac{d_u({h_w}^*)}{d_y({h_w}^*)} \tag{34}$$

The wall yield displacement, $d_y({h_w}^*)$, is obtained from a pushover analysis of the MDOF system subjected to an inverse triangular load distribution representative of the first mode displacement. If the effective modal height is not a multiple of the storey height, displacements are evaluated through linear interpolation between the displacements at the storeys immediately above and below ${h_w}^*$. The ductility of the MDOF frame system, μ_f, is defined as the maximum interstorey drift ductility. At each iteration the interstorey drift ductility is calculated as the maximum ratio of the ultimate drift, $d_{u,f,i}$, to the yield drift, $d_{y,f,i}$, among the n_s storeys divided by the storey height, h_s.

$$\mu_f = \mu_{IDR} = max\left(\frac{\frac{d_{u,f,i}}{h_s}}{\frac{d_{y,f,i}}{h_s}}\right) = max\left(\frac{d_{u,f,i}}{d_{y,f,i}}\right) \tag{35}$$

The yield drift of frames for the *i-th* storey, $d_{y,f,i}$, is the analytical yield displacement given by:

$$d_{y,f,i} = \frac{V_{y,f,i}}{\frac{12E_{c,f}I_{f,y}}{{h_s}^3}} = \frac{\frac{M_{y,f,i}}{h_s/2}}{\frac{12E_{c,f}I_{f,y}}{{h_s}^3}} = \frac{M_{y,f,i}{h_s}^2}{6E_{c,f}I_{f,y}} \tag{36}$$

where $V_{y,f,i}$ and $M_{u,f,i}$ are the yield shear and moment of the frame column at the *i-th* storey.

3) The base shear of the SDOF system at the maximum target ductility capacity, $V_{b,SDOF,w}(\mu = {\mu_w}^*)$ or $V_{b,SDOF,f}(\mu = {\mu_f}^*)$, is computed by iteration on the yield moment of the SDOF system's base hinge, when subjected to the same ground motion and same scale factor of step 2, until the ductility, μ, of the SDOF structure is equal to the target ductility ${\mu_w}^*$ or ${\mu_f}^*$ within a 5% tolerance error. The yield displacements, $d_y({h_w}^*)$ and $d_{y,f}$, are identified as the top displacement corresponding to the yield moment, $M_{y,w}$, or the yield shear, $V_{y,f}$, at the base hinge, respectively.
4) The elastic SDOF system's base shear, $V_{b,SDOF,w}(\mu = 1)$ or $V_{b,SDOF,f}(\mu = 1)$, is computed for the elastic SDOF system when subjected to the same ground motion and same scale factor of step 2.
5) The ductility reduction factor for the SDOF wall system, $R_{\mu,SDOF,w}$, the ductility reduction factor for the MDOF wall system, $R_{\mu,MDOF,w}$, and the modification factor for wall system, $R_{M,w}$, are computed. $R_{\mu,SDOF,f}$, $R_{\mu,SDOF,f}$, $R_{M,f}$ are computed by an approach similar to the wall system.

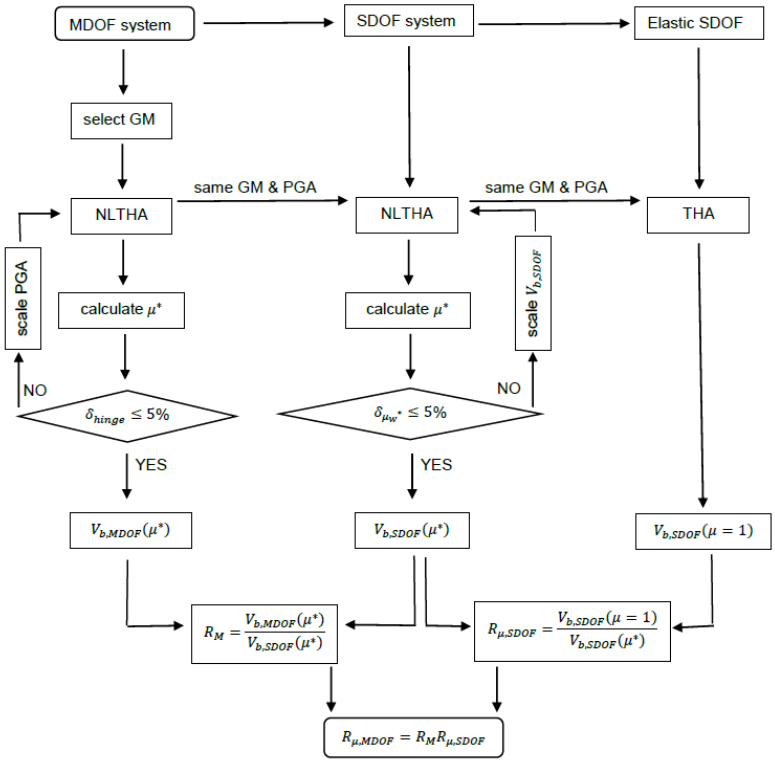

Figure 5: Flowchart for the calculation of the ductility reduction factor. NLTHA: NonLinear Time History Analysis; THA: Time History Analysis; PGA: peak ground acceleration.

4. Analyses and results

Three series of analyses have been carried out for wall systems and three for frame systems. Each analysis evaluated the ductility reduction factor for SDOF and MDOF system and the corresponding modification factor.

The material properties used in the analyses, were: concrete compressive strength $f_c = 38.0\ MPa$; steel yield stress $f_{y,s} = 550.0\ MPa$; steel tensile strength $f_{u,s} = 632.5\ MPa$; steel Young's modulus $E_s = 200\ GPa$; maximum rebar diameter $d_{bl} = 20\ mm$. Structural RC member weight was assumed equal to $25.0\ kN/m^3$. The mean mechanical properties were used in the analytical procedure.

Storey gravity loads in the seismic load combination, q_E, was equal to $7.8\ kN/m^2$ on a influence area of $25.0\ m^2$, assuming a bay length, l_b, of $5.0\ m$ and a storey span, i_b, of $5.0\ m$.

Nonlinear Time History Analyses (NLTHA) were performed to compute the ductility reduction factor in Section 4 and to compare the results of the proposed formulation and the values provided by Eurocode 8 in Section 5. For each structure, a set of 34 natural ground motions were run. A total of 1020 NLTHAs were computed for wall and frame systems. The natural ground motions were the same as those used by [46]. They were selected from the PEER [47] ground motion database. For the MDOF systems, Rayleigh damping matrix was assigned by considering a damping coefficient $\zeta = 5\%$ to the first two modes [40]. For the SDOF systems, a damping coefficient $\zeta = 5\%$ was assigned through the initial stiffness matrix. The analysis time step was defined as the minimum value between $T_1/20$, the time step of the ground motion data and 0.02 seconds. The unconditionally stable Newmark method [48] with constant average acceleration was used ($\gamma = 0.5$ and $\beta = 0.25$).

4.1. Wall structures

Three series of wall structures were taken into consideration, and they are labeled “W1”, “W2” and “W3”, respectively. Each series is composed of 10 systems, with a number of storeys, n_s, ranging from 3 to 12 in storey height $h_s = 3.50\ m$. They all had the same wall section sizes: section thickness $b_w = 0.30\ m$ and section length $l_w = 2.10\ m$. The difference between the series lays in the sectional ductility, equal to 9.3, 11.7 and 14.0 for the three groups, respectively.

Results for wall systems W1, W2 and W3 are illustrated in Figure 6, where numerical results are compared to the proposed analytical results. In the figures numerical results given by OpenSees [43] and analytical predictions are indicated with “OS” and “AN” labels respectively. The Figures 6 graphs show that the analytical prediction for ductility reduction factor, $R_{\mu,MDOF,w}$, modification factor, $R_{M,w}$, and target ductility, ${\mu_w}^*$, were in adequate agreement with respective numerical mean values (OS^{mean}); data dispersion is evidenced through the range of entire population (100%) and the range of 68% coverage of population.

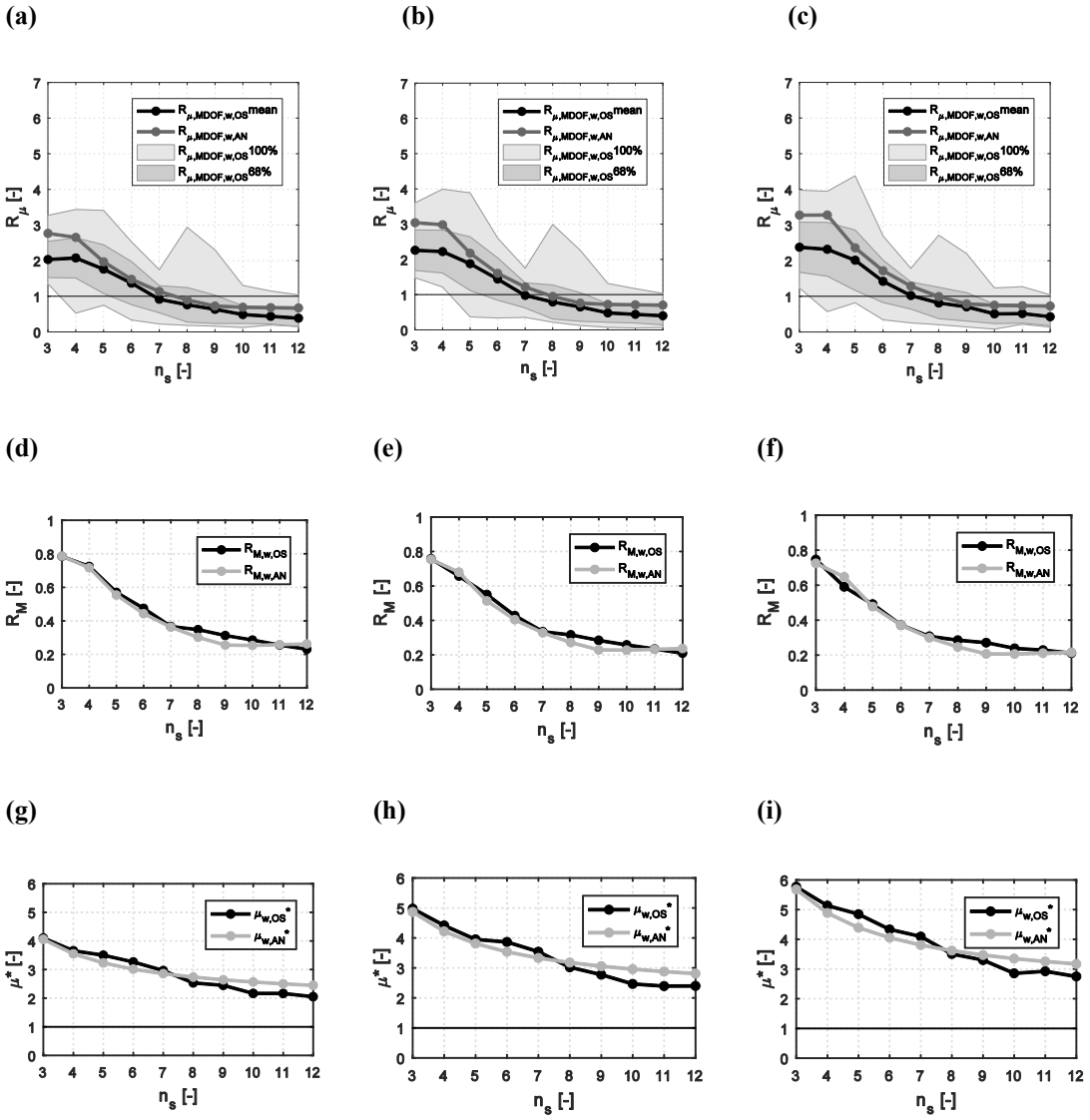

Figure 6: Ductility reduction factor for walls (a): W1, (b): W2, (c): W3, modification factor for walls (d): W1, (e): W2, (f): W3, target ductility for walls (d): W1, (e): W2, (f): W3.

The ductility reduction factor for the MDOF systems, $R_{\mu,MDOF,w,OS}$, was overestimated by the proposed analytical model, $R_{\mu,MDOF,w,AN}$, with an average error of 33%. The modification factor, $R_{M,w,OS}$, was well predicted by the proposed analytical model, $R_{M,AN}$, and it was underestimated with an average error of 5%. The target ductility, ${\mu_{w,OS}}^*$, was well predicted by the proposed analytical model, ${\mu_{w,AN}}^*$, and it was overestimated with an average error of 4%.

The data dispersion was considerable when all analyses are considered, but a lower scatter was demonstrated when 68% coverage of population was considered. It's noteworthy that some convergence problems occurred during the numerical analysis due to convergence failures in the numerical procedure used to calculate the ductility reduction factors, more specifically when the convergence errors exceeded the 5% tolerance in the search for the ground motion scale factor (MDOF system) or the target ductility (equivalent SDOF system) within 20 iterations. The percentage of successful analyses, which is the ratio between successful and total number of analyses, was equal to 92%. Failed analyses are not included in the results. Analyses failed randomly with the number of storeys and the ground motions; they didn't show systematic bias due to certain patterns.

It is evident from Figure 6 that the ductility reduction factor, $R_{\mu,MDOF,w}$, the modification factor, $R_{M,w}$, and the target ductility, ${\mu_w}^*$ decrease with the number of storeys; $R_{\mu,MDOF,w}$ and $R_{M,w}$ are not significantly different among the groups W1, W2 and W3. This result follows the system's loss of capability to exploit the base sectional inelasticity and the increase in the increased importance of higher mode effects with the number of storeys.

Also worthy to note for high numbers of storeys, the ductility reduction factor, $R_{\mu,MDOF,w}$, is less than 1, which means that the system is unable to exploit the base sectional inelasticity and the structure should be designed elastically. Values of $R_{\mu,MDOF,w}$ are ranging from 2.0 to 0.4; from 2.3 to 0.4 and from 2.4 and 0.4 for W1, W2 and W3, respectively.

The modification factor, $R_{M,w}$, decreases with the number of storeys, which means that the higher mode effects progressively increase the base shear in MDOF systems. Values of $R_{M,w}$ are ranging from 0.8 to 0.2 for all groups of walls, then $R_{M,w}$ is slightly affected by the wall's sectional ductility capacity and is mainly controlled by n_s.

The target ductility, ${\mu_w}^*$, decreases with the number of storeys, i.e. the system is less efficient to exploit the sectional ductility and to convert it into available ductility capacity, ${\mu_w}^*$, as n_s increases. Values of ${\mu_w}^*$, are ranging from 4.1 to 2.5, from 4.9 to 2.8 and from 5.7 and 3.2 for W1, W2 and W3, respectively. The increase of ${\mu_w}^*$ from W1 to W3 groups is obvious because the sectional ductility of the walls are 9.3, 11.7 and 14.0 for W1, W2 and W3, respectively.

The comparison of fundamental periods given by the numerical model, $T_{1,w,OS}$, and the analytical model, $T_{1,w,AN}$, given by Equation (10), is reported in Table 1. The analytical fundamental periods underestimate the numerical ones by 14% on average. The scatter between numerical and analytical periods is due to the fact that the analytical formula is developed for uniformly distributed mass systems; on the contrary, the numerical period is computed for lumped mass systems.

Table 1: Fundamental period of wall structures.

	3	4	5	6	7	8	9	10	11	12
$T_{1,w,OS}$ [s]	0.46	0.77	1.15	1.61	2.14	2.76	3.45	4.21	5.06	5.98
$T_{1,w,AN}$ [s]	0.34	0.61	0.96	1.38	1.87	2.45	3.10	3.82	4.63	5.51
Diff.	-25%	-20%	-17%	-14%	-13%	-11%	-10%	-9%	-9%	-8%

4.2. Frame structures

Concerning frame systems, three series of frame structures were taken into consideration and labeled "F1", "F2" and "F3", respectively. Each series was composed of 10 systems, with a number of storeys, n_s, ranging from 3 to 12 and a constant storey height $h_s = 3.50\ m$. They had the same section sizes of the base columns: section width $b_c = 0.40\ m$ and section depth $h_c = 0.40\ m$. The difference between the series lay in the first storey sectional ductility ranges between 3.4-9.2, 2.6-6.9 and 1.7-4.6 for number of storeys ranging from 3 to 12 for the three groups, respectively, due to the increasing axial load.

Results of frame systems F1, F2 and F3 are illustrated below in Figure 7, where numerical results are compared to the proposed analytical results. Numerical results given by OpenSees [43] and analytical predictions are indicated with "OS" and "AN" labels respectively in the graphs. Figures 6 show that the analytical prediction for ductility reduction factor, $R_{\mu,MDOF,f}$, modification factor, $R_{M,f}$, and target ductility, ${\mu_f}^*$, are in good agreement with respective numerical mean values (OS^{mean}); data dispersion was demonstrated through the range of entire population (100%) and range of 68% coverage of population.

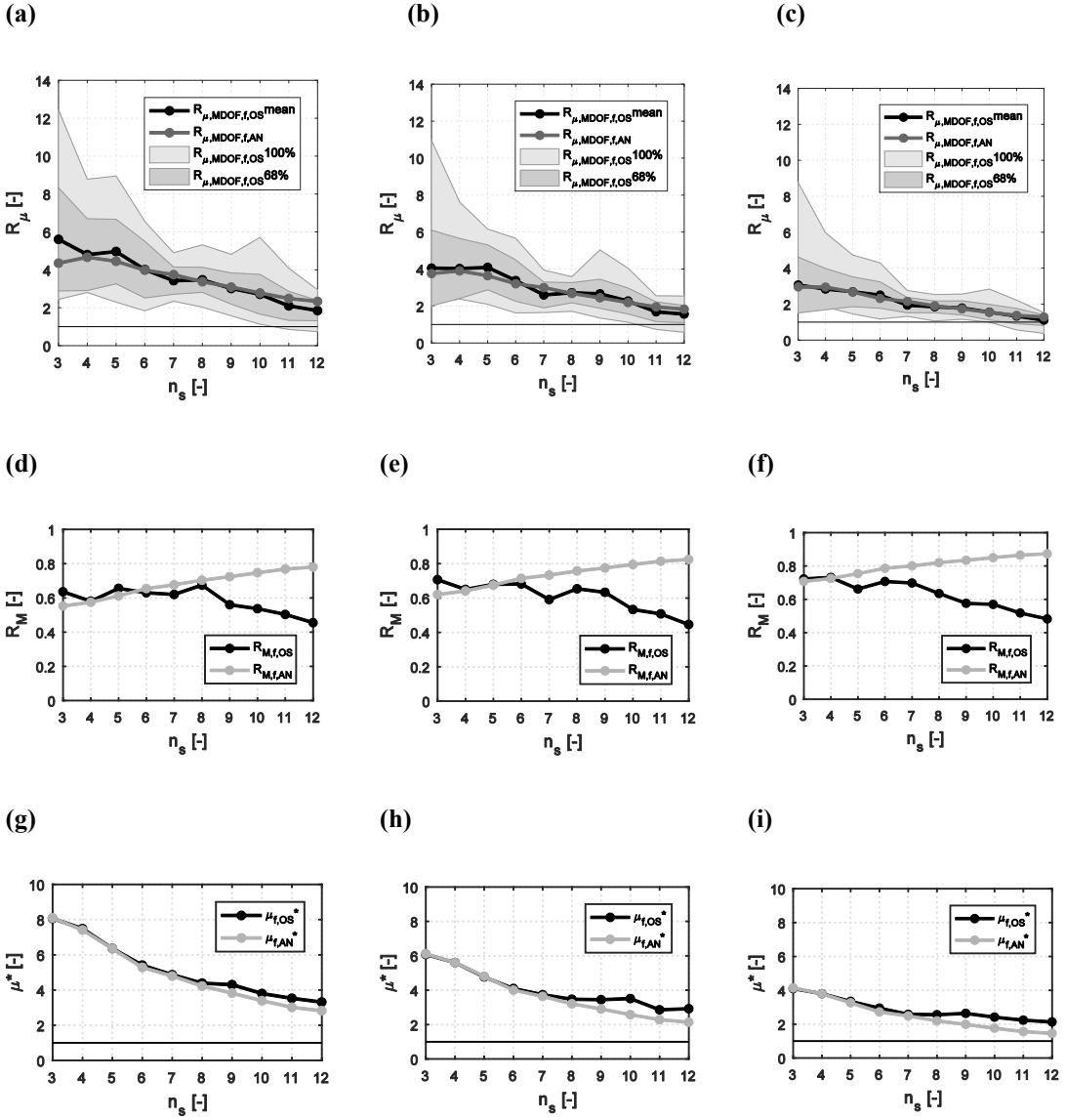

Figure 7: Ductility reduction factor for frames (a): F1, (b): F2, (c): F3, modification factor for frames (d): F1, (e): F2, (f): F3, target ductility for frames (d): F1, (e): F2, (f): F3.

The ductility reduction factor for the MDOF systems, $R_{\mu,MDOF,f,OS}$, was well predicted by the proposed analytical model, $R_{\mu,MDOF,f,AN}$, and was overestimated with an average error of 2%. The modification factor, $R_{M,f,OS}$, was overestimated by the proposed model, $R_{M,f,AN}$, with an average error of 25% and even

higher scatter occurs for high number of storeys. The target ductility, $\mu_{f,OS}{}^{*}$, was underestimated by the proposed model, $\mu_{f,AN}{}^{*}$, with an average error of 10%.

The data dispersion was considerable when all analyses are considered, but a lower scatter was demonstrated when 68% coverage of population was considered. The percentage of successful analyses, which is the ratio between successful and total number of analyses, was equal to 76%. Failed analyses are not included in the results. Analyses failed randomly with the number of storeys and the ground motions; they didn't show systematic bias due to certain patterns.

It is evident from Figure 7 that the ductility reduction factors, $R_{\mu,MDOF,f}$, decrease with the number of storeys following a linear trend, due to the loss of system's capability to exploit the sectional inelasticity. Furthermore, $R_{\mu,MDOF,f}$ is significantly higher than $R_{\mu,MDOF,w}$, especially for a high number of storeys, and $R_{\mu,MDOF,w}$ decreases more rapidly than $R_{\mu,MDOF,f}$. Values of $R_{\mu,MDOF,f,OS}$ are ranging from 5.6 to 1.9, from 4.1 to 1.6 and from 3.1 and 1.1 for F1, F2 and F3, respectively; $R_{\mu,MDOF,f}$ is significantly different among the F1, F2 and F3 groups, unlike what is observed for wall systems.

The modification factor, $R_{M,f}$, does not significantly vary among the groups, unlike the case of wall systems. $R_{M,f}$, is basically constant and slightly affected by both the base column sectional ductility capacity and the number of storeys. Values of $R_{M,f}$ are ranging from 0.7 to 0.4 for all group of frames.

The target ductility, $\mu_f{}^{*}$, decreases with the number of storeys, because the system is less efficient in exploiting sectional ductility and in converting it into available ductility capacity, $\mu_f{}^{*}$, with the increase of n_s. The decrease of $\mu_f{}^{*}$ follows the base column sectional ductility decrease from F1 to F3 groups. Values of $\mu_f{}^{*}$ are ranging from 8.1 to 3.3, from 6.1 to 2.9 and from 4.1 and 2.1 for F1, F2 and F3, respectively.

Table 2 compares the fundamental periods given by the numerical model, $T_{1,f,OS}$, and the analytical model, $T_{1,f,AN}$, given by Equation (23). The analytical fundamental periods overestimate the numerical ones by 11% on average. The scatter between numerical and analytical periods is due to the analytical formula which is developed for uniformly distributed mass systems. On the contrary, the numerical period is computed for lumped mass systems.

Table 2: Fundamental period of frame structures.

	3	4	5	6	7	8	9	10	11	12
$T_{1,f,OS}$ [s]	0.60	0.76	0.93	1.11	1.30	1.49	1.69	1.89	2.10	2.30
$T_{1,f,AN}$ [s]	0.63	0.84	1.05	1.26	1.47	1.68	1.89	2.10	2.31	2.53
Diff.	6%	10%	13%	14%	14%	13%	12%	11%	10%	10%

5. Comparison of the proposed formulations and Eurocode 8

Three couples of design examples for both wall and frame system structures have been developed to compare the performance of the proposed analytical formulation and Eurocode 8 [34] design method. Structures are designed following Eurocode 8 requirements for medium ductility class (DCM) but employing different force reduction factors. Moreover, Eurocode 8 imposes capacity design rules in order to avoid brittle mechanisms such as shear failure in walls, beams and columns.

To perform numerical analyses, the commercial FEM code Midas/Gen [49] was used. Concentrated plasticity models are considered and bilinear diagrams for inelastic hinges are used.

The inelastic hinges' capacity is evaluated at the life-safety limit state with a 10% probability of exceedance in 50 years. The implemented demand spectrum is representative of an Italian seismic zone with a high seismic hazard ($PGA = 0.319g$ on bedrock).

All structural elements are checked for ductile failure modes only, because brittle failures should be excluded by the capacity design. Ductile flexural failure is reached when the rotation of the end inelastic hinges reaches the rotational capacity, defined as 75% of the ultimate chord rotation. Ultimate and yielding chord hinge rotations are evaluated with the equations formulated by [50], [51], [52].

The seismic performance of structures is assessed by means of both Pushover according to the N2 method [53] and NLTHAs analyses.

The displacement performance ratio, γ_d, provided by the N2 method is:

$$\gamma_d = \frac{{d_c}^*}{{d_d}^*} \tag{37}$$

where ${d_c}^*$ is the ultimate displacement of the bilinearised SDOF curve, which is the displacement capacity of the system, and ${d_d}^*$ is the inelastic displacement demand computed from the Acceleration-Displacement Response Spectrum.

The performance ratio in term of peak ground acceleration (PGA), ${\alpha_{N2}}^*$, provided by the N2 method is given by:

$${\alpha_{N2}}^* = \frac{PGA_{c,N2}}{PGA_d} \tag{38}$$

where $PGA_{c,N2}$ is the peak ground acceleration that yields the structure to failure and PGA_d is the peak ground acceleration demand required by the pseudo-acceleration spectrum. The $PGA_{c,N2}$ is calculated iteratively scaling the PGA and consequently the demand spectrum in order to reach the structural capacity with an error tolerance of 1e-6. ${\alpha_{N2}}^*$, is herein introduced to obtain a coherent comparison with NLTHA results. In fact, N2 method is a displacement-based approach and the introduction of ${\alpha_{N2}}^*$ allows to convert the displacement performance to PGA performance.

The performance ratio in terms of PGA, ${\alpha_{TH}}^*$, provided by the NLTHA is given by:

$${\alpha_{TH}}^* = \frac{PGA_{c,TH}}{PGA_d} \tag{39}$$

where $PGA_{c,TH}$ is the peak ground acceleration that causes the structure to failure and PGA_d is the peak ground acceleration demand required by the pseudo-acceleration spectrum. The $PGA_{c,TH}$ is calculated iteratively scaling the PGA and consequently the demand spectrum which is used to select the set of seven compatible ground motions.

The ground motions used in this study are selected by REXEL software [54]. REXEL allows to search for sets of 7 records compatible on the average with given design spectra, according to rules derived from Eurocode 8 [34]. Records may also reflect the sources' seismogenic features in terms of magnitude and epicentral distance, ground motion intensity measures, and soil conditions appropriate to the site. The datasets contained in REXEL are the European Strong-motion Database (ESD), the ITalian ACcelerometric Archive (ITACA) and the Selected Input Motions for displacement-Based Assessment and Design (SIMBAD).

The investigated structures present a number of storeys $n_s = 4, 8, 12$ with constant storey height $h_s = 3.50\ m$. Wall structures are labeled "W4", "W8", "W12" and frame structures "F4", "F8", "F12", respectively. Here below, structures designed using the force reduction factors provided by the proposed analytical formulation and by Eurocode 8 [34] are labeled as "AN" and "EC", respectively. Schematic representations of the wall and frame structures are reported in Figure 8.

Material properties, gravity loads and storey dimensions have been described in Section 4 but material safety factors of the design process were assigned according to Eurocode 8 [34].

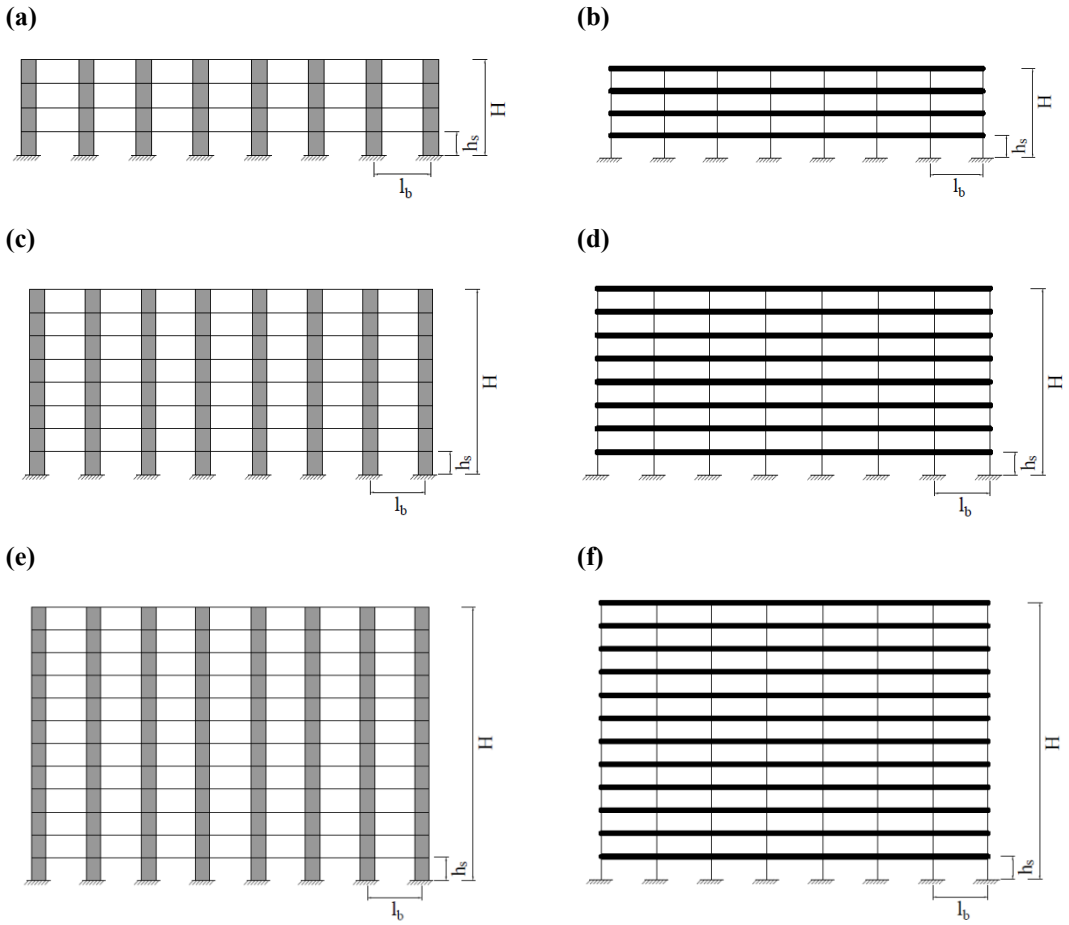

Figure 8: Schematic representations of the studied wall and frame structures, (a): W4, (b): F4, (c): W8, (d): F8, (e): W12, (f): F12.

5.1. Wall structures

The RC wall structures are made of eight walls linked by pinned-pinned rigid beams. Geometrical properties and reinforcement detailing are reported in Table 3, where b_w is the base thickness, l_w is the base length of each wall, Ø is the implemented bars diameter, s is the bar spacing and n the number of bars. The concrete cover is 50 mm for all walls. It is noted that the same section is used for the walls designed following both Eurocode 8 [34]and the proposed formulation, while the reinforcement changes in order to provide the required structural strength.

Force reduction factors provided by Eurocode 8 [34] and by the proposed formulation are reported in Table 4. As mentioned above, the overstrength-dependent component, R_s, of the force reduction factor is not addressed in this study and, for the purpose of this research, R_s is evaluated by means of nonlinear static analyses (pushover analysis). It is noted that when the force modification factor provided by the proposed formulation is lower than 1, it means that the structure has to be designed elastically and $R = 1$. When R is lower than 1, it is shown within round brackets in Table 4.

Performances of wall systems are reported in Table 5, where γ_d, ${\alpha_{N2}}^*$ and ${\alpha_{TH}}^*$ are defined by equations (37), (38) and (39), respectively. A comparison of performance ratios for wall structures is listed in Table 6. It is worth recalling that the structure is safely designed for performance ratios equal or higher than 1.

Table 3: Reinforcement of walls.

ID	Dimensions		Confined end vertical reinforcement			Vertical reinforcement		Horizontal reinforcement	
	b_w $[m]$	l_w $[m]$	n	Ø $[mm]$	s $[mm]$	Ø $[mm]$	s $[mm]$	Ø $[mm]$	s $[mm]$
$W4_{AN}$	0.20	1.00	6	30	100	12	200	12	90
$W4_{EC}$	0.20	1.00	4	20	100	12	200	12	90
$W8_{AN}$	0.30	1.50	12	32	100	12	200	12	90
$W8_{EC}$	0.30	1.50	4	24	100	12	200	12	90
$W12_{AN}$	0.35	2.00	10	32	100	12	200	12	90
$W12_{EC}$	0.35	2.00	8	26	100	12	200	12	90

Table 4: Force reduction factors for wall structures.

	$W4_{AN}$	$W4_{EC}$	Diff.	$W8_{AN}$	$W8_{EC}$	Diff.	$W12_{AN}$	$W12_{EC}$	Diff.
R_μ, q_0	1.39	3.00	+116%	0.68	3.00	+344%	0.66	3.00	+356%
R_s, α_u/α_1	1.08	1.00	-8%	1.08	1.00	-8%	1.09	1.00	-9%
R, q	1.50	3.00	+100%	1.00 (0.73)	3.00	+200%	1.00 (0.72)	3.00	+200%

Table 5: Performance ratios for wall structures.

	$W4_{AN}$	$W4_{EC}$	Diff.	$W8_{AN}$	$W8_{EC}$	Diff.	$W12_{AN}$	$W12_{EC}$	Diff.
γ_d	0.92	0.59	-36%	1.20	0.62	-48%	1.08	0.81	-25%
α^*_{N2}	0.88	0.50	-44%	1.43	0.54	-62%	1.07	0.82	-23%
α^*_{TH}	0.95	0.69	-27%	1.49	0.74	-50%	1.00	0.89	-11%

Table 6: Comparison of performance ratios for wall structures.

	$W4_{AN}$	$W4_{EC}$	$W8_{AN}$	$W8_{EC}$	$W12_{AN}$	$W12_{EC}$
$(\alpha^*_{N2} - \alpha^*_{TH})/\alpha^*_{TH}$	-7%	-28%	-4%	-28%	+8%	-8%
$(\gamma_d - \alpha^*_{N2})/\alpha^*_{N2}$	+5%	+19%	-16%	+15%	+0%	-2%

As clearly shown in Table 4, force reduction factors provided by Eurocode 8 [34] are significantly higher than those calculated with the proposed formulation. Consequently, as reported in Table 5, the Eurocode 8 yields unsafe and underdesigned structures, particularly for low and mid-rise buildings, these have smaller fundamental periods falling in the constant acceleration plateau of the design spectrum, where structures are subjected to the highest seismic demand. Value differences of R lead to considerable variations in performance ratios even with respect to structures with longer periods (that fall into the descending branch of the design spectrum).

The comparison between α^*_{N2} and α^*_{TH} reported in Table 6, generally shows small differences. It can be concluded that for regular wall structures the N2 method is an effective tool to assess the structural performance. Furthermore, the comparison between γ_d and α^*_{N2} shows that displacement ratios are very close to ratios in terms of PGA, thus γ_d provides a reliable performance assessment and the calculation of α^*_{N2} can be avoided.

5.2. Frame structures

The RC frames have seven bays. Geometrical properties and reinforcement details are listed in Table 7 and Table 8, where b_c and h_c are the base columns' width and depth, respectively; b_b and h_b are the beams width and depth, respectively, Ø is the implemented bars diameter, s is the bar spacing, n the number of bars. n *total* is the total number of bars in the column section and n *top-bottom* is the number of bars along b_c, which are the section sides perpendicular to flexure direction. Finally, concrete cover is 60 mm for all beams and columns.

Force reduction factors provided by Eurocode 8 [34] and by the proposed formulation are reported in Table 9. The performances of frame systems are reported in Table 10. A comparison of performance ratios for frame structures is listed in Table 11.

Table 7: Reinforcement of columns.

ID	Dimensions		Longitudinal reinforcement			Stirrups		
	b_c $[m]$	h_c $[m]$	*n total*	Ø $[mm]$	*n top-bottom*	n	Ø $[mm]$	s $[mm]$
$F4_{AN}$	0.40	0.40	12	22	4	3	10	100
$F4_{EC}$	0.40	0.40	16	22	5	3	10	100
$F8_{AN}$	0.45	0.45	20	22	6	3	10	50
$F8_{EC}$	0.45	0.45	20	22	6	3	10	50
$F12_{AN}$	0.50	0.50	24	22	7	3	10	60
$F12_{EC}$	0.50	0.50	24	22	7	3	10	60

Table 8: Reinforcement of beams.

ID	Dimensions		Top reinf.		Bottom reinf.		Stirrups		
	b_b $[m]$	h_b $[m]$	n	Ø $[mm]$	n	Ø $[mm]$	n	Ø $[mm]$	s $[mm]$
$F4_{AN}$	0.40	0.30	8	18	8	18	2	10	50
$F4_{EC}$	0.40	0.30	8	20	8	20	2	10	50
$F8_{AN}$	0.40	0.30	9	22	9	22	2	10	50
$F8_{EC}$	0.40	0.30	9	22	9	22	2	10	50
$F12_{AN}$	0.40	0.35	8	24	8	24	2	10	60
$F12_{EC}$	0.40	0.35	8	24	8	24	2	10	60

Table 9: Force reduction factors for frame structures.

	$F4_{AN}$	$F4_{EC}$	Diff.	$F8_{AN}$	$F8_{EC}$	Diff.	$F12_{AN}$	$F12_{EC}$	Diff.
R_μ, q_0	4.30	3.00	-30%	3.93	3.00	-24%	3.02	3.00	-1%
R_s, α_u/α_1	1.93	1.30	-34%	1.49	1.30	-12%	1.22	1.30	+6%
R, q	8.48	3.90	-54%	5.84	3.90	-33%	3.68	3.90	+6%

Table 10: Performance ratios for frame structures.

	$F4_{AN}$	$F4_{EC}$	Diff.	$F8_{AN}$	$F8_{EC}$	Diff.	$F12_{AN}$	$F12_{EC}$	Diff.
γ_d	0.86	0.99	+14%	0.98	0.98	0%	1.87	1.87	0%
α^*_{N2}	0.80	0.98	+22%	0.98	0.98	0%	1.77	1.77	0%
α^*_{TH}	1.00	1.04	+5%	1.05	1.05	0%	1.91	1.91	0%

Table 11: Comparison of performance ratios for frame structures.

	$F4_{AN}$	$F4_{EC}$	$F8_{AN}$	$F8_{EC}$	$F12_{AN}$	$F12_{EC}$
$(\alpha^*_{N2} - \alpha^*_{TH})/\alpha^*_{TH}$	-19%	-6%	-7%	-7%	-7%	-7%
$(\gamma_d - \alpha^*_{N2})/\alpha^*_{N2}$	+7%	+1%	0%	0%	0%	0%

As clearly shown in Table 9, force reduction factors provided by Eurocode 8 [34] are lower or similar to those calculated with the proposed formulation, suggesting that the Eurocode 8 option should yield overdesigned structures. However, capacity design rules don't allow exploitation of the higher force reduction factor provided by the proposed formulation. Consequently, as reported in Table 10, the design of frame structures – except for low-rise buildings – is mainly controlled by beam design and therefore demand for columns is straightforward following the "weak beam / strong column" capacity design rule.

Similarly to wall structures, the comparison of α^*_{N2} with α^*_{TH} reported in Table 11 generally shows slight differences and demonstrates that for regular frame structures the N2 method is an effective simplified tool

to assess the structural performance. Furthermore, the comparison of γ_d with α_{N2}^* shows that displacement ratios are very close to ratios in terms of PGA, thus γ_d provides a reliable performance assessment and the calculation of α_{N2}^* can be avoided.

6. Summary and conclusions

In the present work, an analytical formulation to estimate the ductility force reduction factor is proposed for wall and frame structures. Key points of the study are summarised in the following:

1) The proposed analytical models for wall and frame structures consist of a single linear elastic cantilever beam with a rotational plastic hinge at the base and a linear elastic one-storey/one-column shear frame with two rotational plastic hinges, one at the base and one at the top of the column, respectively. The wall and frame systems are modelled as a flexural beam and a shear frame with a single column/storey, respectively.
2) In terms of input data, the proposed analytical models only require the structural yield and ultimate displacements, geometry and general material properties. The computed displacement ductility is taken as proxy of the ductility reduction factor. Such analytical models allow linking global to local ductility demands and therefore the computed estimate of the force ductility reduction factors. These properties are used to define an equivalent SDOF system [40] in order to achieve the ductility reduction factor. The modification factor is estimated by analytical expressions [42], which take into account higher mode effects on the base shear. Once the modification factor is known, the ductility reduction factor of MDOF systems is obtained from the ductility reduction factor of SDOF systems.
3) Three levels of sectional ductility are investigated for both wall and frame structures. Structures with a number of storeys ranging from 3 to 12 are considered, representative of low- to mid-rise buildings. To validate the applicability of the proposed formulation, a database of 34 natural ground motions was selected and a total of 1020 nonlinear time history analyses were carried out. An iterative procedure was implemented in order to calculate the ductility reduction factors and the modification factors. Results of wall and frame systems show good agreement between ductility reduction factors provided by the analytical model and by numerical analyses.
4) For wall systems, the ductility reduction factors for MDOF systems and modification factors decrease with the number of storeys. The study highlights the loss of system's capability to exploit the base's sectional ductility capacity as well as the importance of higher mode effects with the number of storeys. Finally, the proposed formulation accurately appraises numerical results of ductility reduction factors for wall systems.
5) For frame systems, the ductility reduction factors for MDOF systems decrease with the number of storeys, similarly to wall systems. On the other hand, the modification factor is basically constant and slightly affected by both the sectional ductility capacity of the base column and the number of storeys. Finally, the proposed formulation accurately appraises numerical results of ductility reduction factors for frame systems.
6) Applications to three design examples of wall structures and three of frame structures show that the force reduction factors provided by Eurocode 8 [34] for wall structures are significantly higher than those computed with the proposed formulation and that the force reduction factors provided by Eurocode 8 [34] for frame structures are lower or similar than those calculated with the formulation method. Moreover, the comparison of the three type of performance ratios, $\gamma_d{}^*$, $\alpha_{N2}{}^*$, $\alpha_{TH}{}^*$, show small differences and it can be concluded that for regular structures the N2 method is an effective simplified tool to assess the structural performance.

The force reduction factor mainly depends on the structure's ductility and on the structural overstrength. The current generation of seismic design codes suffers from a several shortcomings; Among these, the fact that the base shear is computed using a pre-defined force reduction factor, which is constant for a given structural system type. Consequently, for the same design input, structures of the same type but different geometry are subjected to different ductility demands and perform differently during an earthquake. The work presented in this paper intends to contribute to the development of revised force-based design guidelines for the next generation of seismic design codes.

Following the developments regarding the ductility reduction factor, future research will be necessary to identify an analytical methods able to assess the overstrength factor in both its main terms of ductility and overstrength. Additional design examples have to be computed to assess reliability of the proposed method application to real case studies and provide a complete statistical comparison to current building codes. Herein, the choice of selecting basic structures is conditioned by the need to perform simple analysis to allow the understanding of the obtained results. Applying the proposed formulation to existing buildings, which are often inadequate with respect to the seismic performance required by modern codes, is recommended in order to assess these structures' seismic vulnerability. The majority of existing buildings were designed for gravity loads only, lacking both earthquake resistance criteria and adequate detailing. Seismic upgrading is fundamental to obtain safer structures, particularly for public buildings strategic to social purposes. A design method applicable to existing structures could lead to suitable retrofit solutions ([55], [56], [57], [58]).

Acknowledgements

The authors wish to acknowledge the support provided by FAR funding from the University of Ferrara, 2016-2017, "Force-Based Seismic Design of Dual System Structures". The first author wishes also to acknowledge the the support provided by "Call for Young Researchers - contributo 5 per mille assegnato all'Università degli Studi di Ferrara - dichiarazione dei redditi dell'anno 2012".

References

[1] Biot MA. Transient Oscillations in Elastic Systems. Ph.D. Thesis No. 259. Aeronautics Department, Calif. Inst. of Tech., Pasadena, CA, US, 1932.
[2] Housner GW. Behaviour of structures during earthquakes. J. Eng. Mech. Div. ASCE 1959; **4**:109-129.
[3] Veletsos AS, Newmark NM. Effect of inelastic behaviour on response of simple system to earthquake motion. Proc. 2nd World Conference on Earthquake Engineering 1960, Tokyo, Japan, 855-912.
[4] Structural Engineers Association of California (SEAOC). Seismic Design Recommendations, Blue Book. SEAOC: Sacramento, CA, US, 1959.
[5] International Conference of Building Officials (ICBO). Uniform building code (UBC). 2nd ed., Vol. 1. ICBO: Los Angeles, CA, US, 1958.
[6] Paulay T, Priestley MJN. Seismic design of reinforced concrete and masonry buildings. New York, NY, US: John Wiley & Sons, Inc.; 1992. 768 p.
[7] Kappos AJ. Evaluation of behaviour factors on the basis of ductility and overstrength studies. Eng. Struct. 1999; **21**(9):823-835.
[8] Applied Technology Council (ATC). Structural response modification factors (ATC-19). ATC: Redwood City, CA, US, 1995.
[9] Santa-Ana PR. Estimation of strength reduction factors for elastoplastic structures: modification factor. 13th WCEE, no. 126. Vancouver, BC, Canada, 2004.
[10] Wang HY, Cai J, Bu GB. Influence of high mode effects on ductility reduction factors for MDOF shear-type structures. International Journal of Advancements in Computing Technology (IJACT) 2013; **5**(9):1150-1157.
[11] Chopra AK. Dynamics of Structures: Theory and Applications to Earthquake Engineering, First Edition. Englewood Cliffs, NJ, US, Pearson Prentice-Hall; 1995. 761 p.
[12] Mwafy AM, Elnashai AS. Calibration of force reduction factors of RC buildings. J. Earthq. Eng. 2002; **6**(2):239-273.
[13] Elnashai AS, Mwafy AM. Overstrength and force reduction factors of multistorey reinforced-concrete buildings. Struct. Design. Tall. Build. 2002; **11**:329-351.
[14] Aydemir ME, Aydemir C. Overstrength factors for SDOF and MDOF systems with soil structure interaction. Earthq. Struct. 2016; **10**(6):1273-1289.
[15] Newmark NM, Hall WJ. Seismic design criteria for nuclear reactor facilities. Report No. 46. Building Practices for Disaster Mitigation, National Bureau of Standards (NBS), Department of Commerce, Gaithersburg, MD, US, 1973:209-236.
[16] Riddel R, Newmark NM. Statistical analysis of response of nonlinear systems subjected to earthquakes. Structural Research Series No. 468. Dept. Of Civ. Engrg., University of Illinois, Urbana, IL, US, 1979.
[17] Lai SP, Biggs JM. Inelastic response spectra for a seismic building design. ASCE J. Struct. Div. 1980; **106**(ST6):1995-1310.
[18] Riddel R, Hidalgo P, Cruz E. Response modification factors for earthquake resistant design of short period structures. Earthq. Spectra. 1989; **5**(3):571-590.
[19] Hidalgo PA, Arias A. New chilean code for earthquake-resistant design of buildings. Proc. 4th U.S. Nat. Conf. Earthquake Engrg. 1990, Palm Springs, CA, US, Vol. 2, 927-936.

[20] Nassar A, Krawinkler K. Seismic Demands for SDOF and MDOF. Report No.95. Dept. of Civil Engineering, Stanford University, Stanford, CA, US, 1991.
[21] Miranda E. Site-dependent strength reduction factors. J. Struct. Eng. 1993; **119**(12):3503-3519.
[22] Vidic T, Fajfar P, Fischinger M. Consistent inelastic design spectra: strength and displacement. Earthq. Eng. Struct. D. 1994; **23**(5):507-521.
[23] Elghadamsi FE, Mohraz B. Inelastic earthquake spectra. Earthq. Eng. Struct. D. 1987; **15**:91-104.
[24] Watanabe G, Kawashima K. An evaluation of the force reduction factor in the force based seismic design. NIST special publication SP 2002. National Institute of Standards and Technology (NIST), Department of Commerce, Gaithersburg, MD, US, 201-218.
[25] Borzi B, Elnashai AS. Refined force reduction factors for seismic design. Eng. Struct. 2000; **22**:1244-1260.
[26] Ordaz M, Perez-Rocha LE. Estimation of strength-reduction factors for elastoplastic systems: A new approach. Earthq. Eng. Struct. D. 1998; **27**(9):889-901.
[27] Vamvatsikos D, Cornell CA. Direct estimation of the seismic demand and capacity of oscillators with multi-linear static pushovers through IDA. Earthq. Eng. Struct. D. 2006; **35**(9):1097-1117.
[28] Miranda E, Bertero VV. Evaluation of strength reduction factors for earthquake-resistant design. Earthq. Spectra. 1994; **10**(2):357-379.
[29] Veletsos AS, Vann WP. Response of ground-excited elasto-plastic systems. J. Struct. Div. ASCE. 1971; **97**(4):1257-1281.
[30] Moghaddam H, Mohammadi RK. Ductility reduction factor of MDOF shear-building structures. J. Earthq. Eng. 2001; **5**(3):425-440.
[31] Santa-Ana PR, Miranda E. Strength reduction factors for multi-degree-of-freedom systems. 12th WCEE, no. 1446. Auckland, AUK, New Zealand, 2000.
[32] Wang H, Cai J, Zhou J. Comparison of ductility reduction factors for MDOF flexure-type and shear-type systems. International Journal of Vibroengineering 2014; **16**(1):231-239.
[33] Gerami, M., Siahpolo, N. and Vahdani, R. Effects of higher modes and MDOF on strength reduction factor of elastoplastic structures under far and near-fault ground motions. Ain Shams Engineering Journal 2017; **8**(2):127-143.
[34] European Committee for Standardization (CEN). Eurocode 8: Design of Structures for Earthquake Resistance. Part 1: General Rules, Seismic Actions and Rules for Buildings (UNI EN 1998-1), CEN: Brussels, Belgium, 2013.
[35] Ministry of Infrastructure and Transport (MIT). Norme tecniche per le costruzioni (DM 14/1/2008). MIT: Rome, Italy, 2008.
[36] American Society of Civil Engineers (ASCE). Minimum design loads for buildings and other structures (ASCE SEI 7-10). ASCE: Reston, VA, US, 2010.
[37] Standards New Zealand. Structural design actions - Part 5: Earthquake actions (NZS 1170.5). Standards New Zealand: Wellington, WGN, New Zealand, 2004.
[38] Building Center of Japan (BCJ). Building Standard Law. BCJ: Tokyo, Japan, 2013.
[39] National Research Council of Canada (NRCC). National Building Code of Canada. NRCC: Ottawa, ON, Canada, 2015.
[40] Chopra AK. Dynamics of Structures: Theory and Applications to Earthquake Engineering, Third Edition. Englewood Cliffs, NJ, US, Pearson Prentice-Hall; 2006. 914 p.
[41] Goel RK, Chopra AK. Period formulas for concrete shear wall buildings. J. Struct. Eng. 1998; **124**(4):426-433.
[42] Priestley MJN, Calvi GM, Kowalsky M. Displacement-based seismic design of structures. Pavia, Italy: IUSS Press; 2007. 721 p.
[43] OpenSees. Open System for Earthquake Engineering Simulation, Version 2.4.5. Pacific Earthquake Engineering Research Center (PEER), CA, US, 2015. http://opensees.berkeley.edu/.
[44] Mazzoni S, McKenna F, Scott MH, Fenves GL. OpenSees command language manual. Open System for Earthquake Engineering Simulation (PEER), University of California, Berkeley, CA, US, 2007. http://opensees.berkeley.edu.
[45] MATLAB. Version R2013a. The MathWorks, Inc., MA, USA, 2013. https://it.mathworks.com/.
[46] Karavasilis TL, Bazeos N, Beskos DE. Bahavior factor for performance-based seismic design of plane steel moment resisting frames. J. Earthq. Eng. 2007; **11**:531-559.
[47] Pacific Earthquake Engineering Research Centre (PEER). Strong Motion Database. PEER: University of California, Berkeley, CA, US, 2005. http://peer.berkeley.edu/.
[48] Bathe KJ. Finite Element Procedures. Upper Saddle River, NJ, US: Pearson Prentice-Hall; 1996. 1037 p.
[49] Midas/Gen, Integrated design system for buildings and general structures, Version 2.1. MIDAS Information Technology Co., Ltd., Seongnam, KR-41 Korea, 2016. https://www.midasuser.com/.
[50] Biskinis D, Fardis MN. Deformations at flexural yielding of members with continuous or lap-spliced bars. Struct. Concrete 2010; **11**(3):127-138.
[51] Biskinis D, Fardis MN. Flexure-controlled ultimate deformations of members with continuous or lap-spliced bars. Struct. Concrete 2010; **11**(2):93-108.
[52] Panagiotakos TB, Fardis MN. Deformations of reinforced concrete members at yielding and ultimate. ACI Struct. J. 2001; **98**(2):135-148.
[53] Fajfar P. A nonlinear analysis method for performance based seismic design. Earthq. Spectra 2000 **16**(3):573-592.
[54] Iervolino I, Galasso C, Cosenza E. REXEL: computer aided record selection for code-based seismic structural analysis. B. Earthq. Eng. 2010; **8**(2):339-362.
[55] Biskinis D, Fardis MN, Upgrading of resistance and cyclic deformation capacity of deficient concrete columns. Geotechnical, Geological and Earthquake Engineering 2009; **10**:307-328.

[56] Biskinis D, Fardis MN. Models for FRP-wrapped rectangular RC columns with continuous or lap-spliced bars under cyclic lateral loading. Eng. Struct. 2013; **57:**199-212.
[57] Fardis MN, Schetakis A, Strepelias E. RC buildings retrofitted by converting frame bays into RC walls, Bull. Earthq. Eng. 2013; **11**(5):1541-1561.
[58] Zerbin M, Aprile A. Sustainable retrofit design of RC frames evaluated for different seismic demand. Earthq. Struct. 2015; **9**(6):1337-1353.